Producing Incident Shortwave Radiation and Photosynthetically Active Radiation Products Over Land Surfaces from MODIS and Multiple Geostationary Satellite Data

Drs. Dongdong Wang, Tao He
Yi Zhang, Meredith Brown
Prof. Shunlin Liang
University of Maryland
May 21 2015

Outline

- Importance of insolation and PAR
- Objective and major tasks
- Progress and current status
- Summary of recent researches
  - Use of hyperspectral data
  - New optimization method
  - Temporal scaling of daily shortwave radiation
- Timetable and future work
- Summary

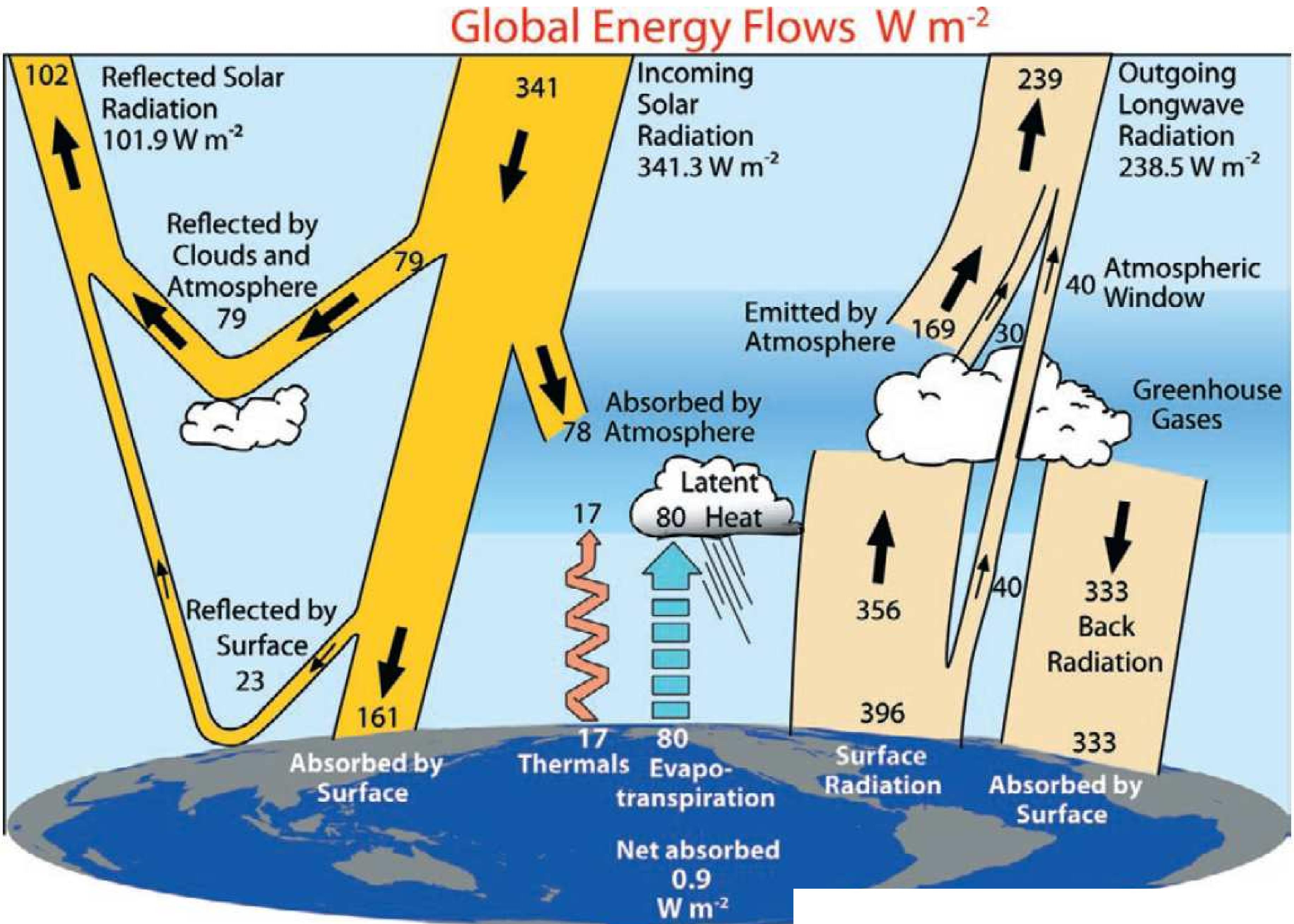

Trenberth et al. (2009)

Need for high spatial resolution products

- Current global radiation products have coarse spatial resolution (>1°) primarily for atmospheric modeling, and do not account for many local features, such as urbanization.
- Land applications require the high spatial resolution (~1km) but the reasonable temporal resolution (e.g., daily):
  - Ecosystem modeling (say, MOD17 NPP product) requires high-resolution products of PAR(1km);
  - Hydrological modeling (ET, MOD16) at 1km;
  - Other applications (e.g., drought monitoring, clean renewable solar energy).

Incident shortwave radiation and PAR products

Current global incident **shortwave radiation** satellite products

Insolation products	Spatial resolution	Temporal resolution	Temporal range
ISCCP	280km	3-hour	1983-2008
GEWEX-SRB	1°	3-hour	1983-2007
CERES	140km	3-hour	1997-present

WMO requirements for surface downward shortwave irradiance

	Uncertainty goal (Wm^{-2})	Uncertainty threshold (Wm^{-2})	Horizontal resolution goal (km)	Horizontal resolution Threshold (km)
Global NWP	1	20	10	100
Agricultural Meteorology	N/A	N/A	1	20
Climate-AOPC	5	10	25	100

Accuracy of current data sets of incident shortwave radiation

R^2, BIAS, RELATIVE BIAS OF SATELLITE PRODUCTS, STD AND RELATIVE STD OF THE DIFFERENCES BETWEEN OBSERVED AND SATELLITE SURFACE DOWNWELLING SHORTWAVE IRRADIANCE (Wm^{-2}) AT ALL SITES FROM 2000–2002

Sites	GEWEX-SRB(AllSky2000-2002)			ISCCP-FD (AllSky2000-2002)			CERES-FSW(AllSky2000-2002)		
	R^2	Bias[a] (%)[b]	STD (%)	R^2	Bias (%)	STD (%)	R^2	Bias (%)	STD (%)
North America									
Bondville	0.91	-6.7(-2.1%)	78.0(25%)	0.89	-12.5(-4%)	83.7(27%)	0.85	14.0(2.7%)	103.2(20%)
Boulder	0.84	-13.5(-4.0%)	107.4(32%)	0.85	-1.9(-0.6%)	106.7(32%)	0.64	9.0(1.5%)	157.0(26%)
Desert_Rock	0.94	-14.2(-3.4%)	74.8(18%)	0.96	-16.2(-3.9%)	62.2(15%)	0.87	20.3(2.9%)	82.0(12%)
Fort_Peck	0.92	-14.6(-5.0%)	70.2(24%)	0.88	-6.5(-2.2%)	84.1(29%)	0.88	18.9(3.8%)	87.9(18%)
Goodwin	0.95	-0.6(-0.2%)	62.5(19%)	0.88	-1.3(-0.4%)	94.5(28%)	0.89	33.9(6.1%)	87.2(16%)
Penn_State	0.92	-0.6(-0.2%)	69.4(24%)	0.90	2.0(0.7%)	78.6(27%)	0.87	37.9(7.8%)	98.7(20%)
Mean	0.91	-8.4(-2.5%)	77.1(24%)	0.89	-6.1(-1.7%)	85.0(26%)	0.83	22.3(4.1%)	102.7(19%)
Tibetan Plateau									
Amdo	0.84	-1.8(-0.5%)	116.9(31%)	0.80	-20.6(-5.4%)	128.5(34%)	0.35	46.5(6.7%)	165.9(24%)
D66	0.87	15.9(4.8%)	88.8(27%)	0.88	24.7(7.5%)	87.7(27%)	0.57	74.9(13.0%)	124.7(22%)
D110	0.85	-44.6(-10%)	131.0(30%)	0.87	-52(-12.1%)	122.8(29%)	0.21	-58.7(-6.8%)	273.9(32%)
Naqu	0.83	-18.0(-4.7%)	125.2(32%)	0.84	-25.9(-6.7%)	121.7(31%)	0.25	10.0(1.4%)	220.6(31%)
Toutouhe	0.86	-18.5(-4.9%)	107.3(29%)	0.86	-15.1(-4.0%)	110.7(30%)	0.36	40.3(6.0%)	189.0(28%)
Mean	0.85	-13.4(-3.1%)	113.8(30%)	0.85	-18.0(-4.1%)	114.4(30%)	0.35	22.6(4.1%)	194.8(27%)
Southeast Asia									
Sukothai	0.80	-90.2(-22%)	153.8(38%)	0.83	-38.9(-9.7%)	138.1(34%)	0.40	-118.8(-15%)	204.9(26%)
TakEgat	0.71	8.2(2.6%)	147.1(47%)	0.77	77.1(24.6%)	141.6(45%)	0.42	107.0(19%)	161.3(28%)
Kogma	0.74	45.8(14.7%)	139.6(45%)	0.77	69.4(23.0%)	137.6(46%)	0.46	125.1(22%)	170.0(30%)
Bukit	0.72	43.4(12.8%)	122.5(36%)	0.68	108.7(32%)	146.1(43%)	0.44	107.5(20%)	161.5(30%)
Palangkaraya	0.79	20.5(5.3%)	113.9(29%)	0.78	65.6(17.1%)	123.0(32%)	0.64	130.7(24%)	110.4(20%)
Sakaerat	0.80	19.0(5.2%)	116.7(32%)	0.81	71.6(19.4%)	119.3(32%)	0.48	83.8(13.5%)	157.0(25%)
Mean	0.76	7.8(3.1%)	132.3(38%)	0.77	58.9(17.7%)	134.3(39%)	0.47	72.6(13.9%)	160.9(27%)

Gui, S., S. Liang, K. Wang, and L. Li, (2010), Validation of Three Satellite-Estimated Land Surface Downward Shortwave Radiation Datasets, *IEEE Geoscience and Remote Sensing Letters*,7(4):776-780

Objective and major tasks

Objective: to produce global high-resolution (5km, 3-hours) incident shortwave radiation and PAR over land surfaces from Terra/Aqua MODIS and a series of geostationary satellite data.

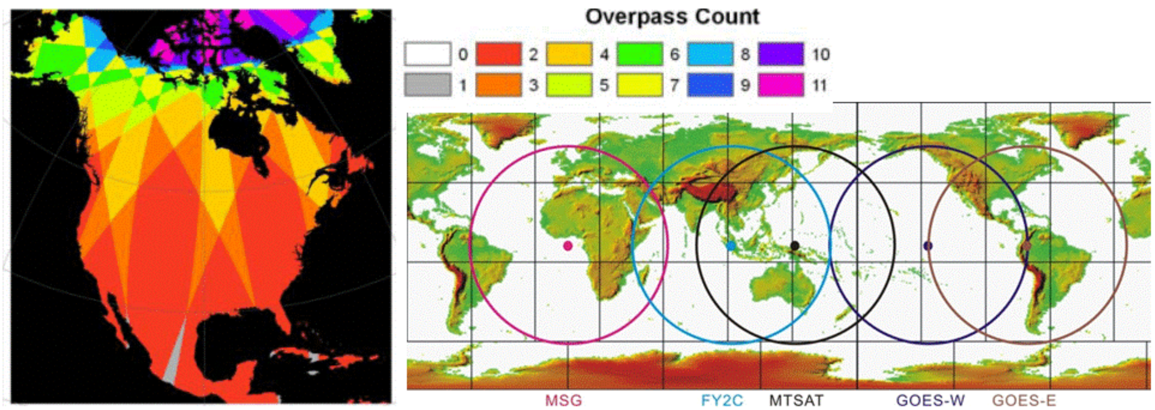

Figure. Daytime MODIS overpass counts from both Terra and Aqua and coverage of the current geostationary satellites.

Major tasks:

1.ATBD improvement and code delivery

2.Evaluation of sensor radiometric calibration

3.Algorithm validation

4.Product quality assessment

5.Product validation

6.Outreach and product advertisement

Algorithms for retrieving PAR and insolation

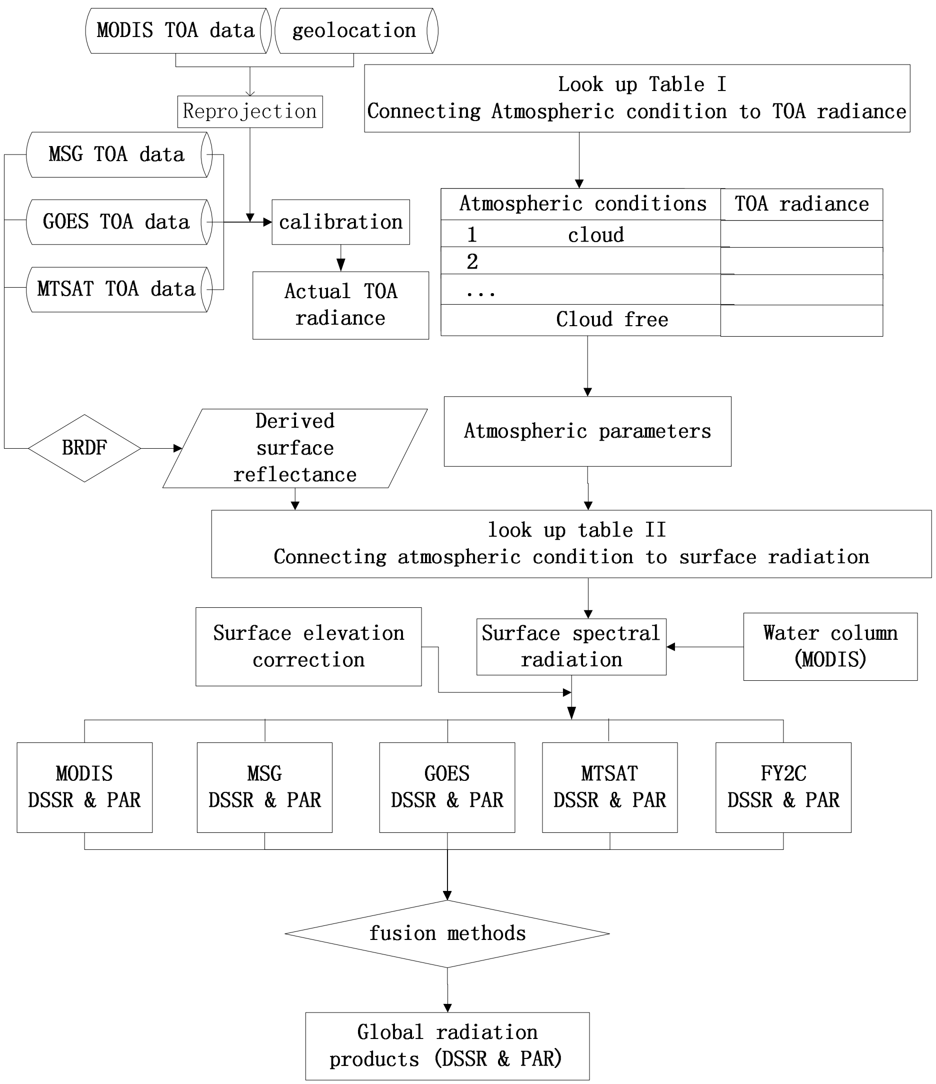

The basic procedure is composed of two steps:

(1) determination of the surface reflectance from observations under the "clearest" atmospheric conditions in a temporal window;

(2) calculation of incident PAR from the determined surface reflectance and TOA radiance/reflectance using the LUT approach.

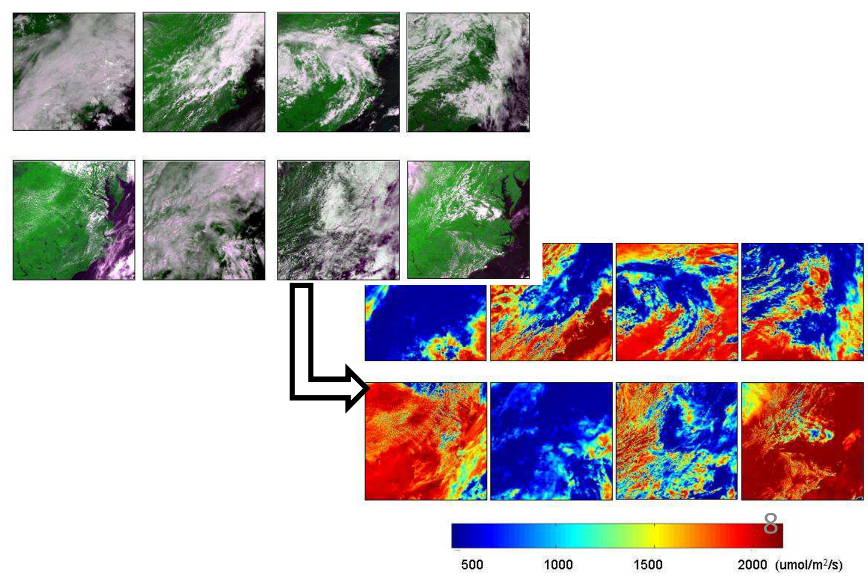

Sensitivity study of the algorithms

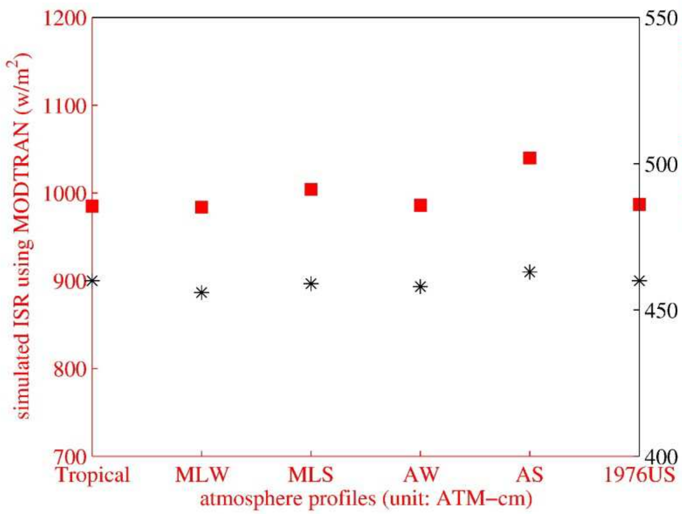

Atmosphere profile

Tropical, MLW, MLS, AW, AS, and 1976US represent the tropical, mid-latitude winter, mid-latitude summer, Arctic winter, Arctic summer, and 1976 US standard atmosphere profiles, respectively.

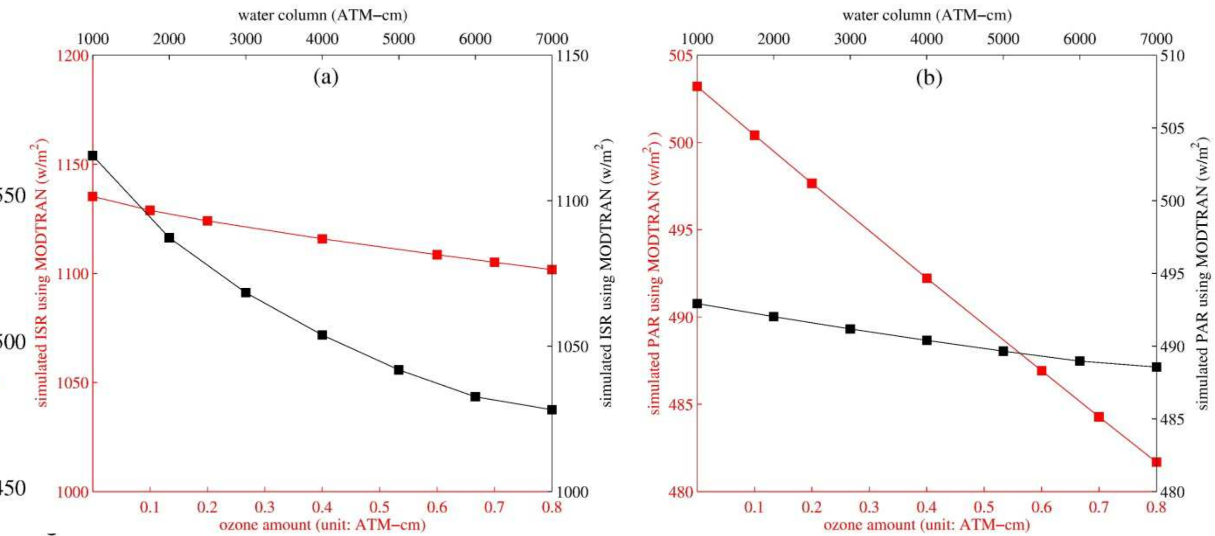

Water vapor and ozone concentration

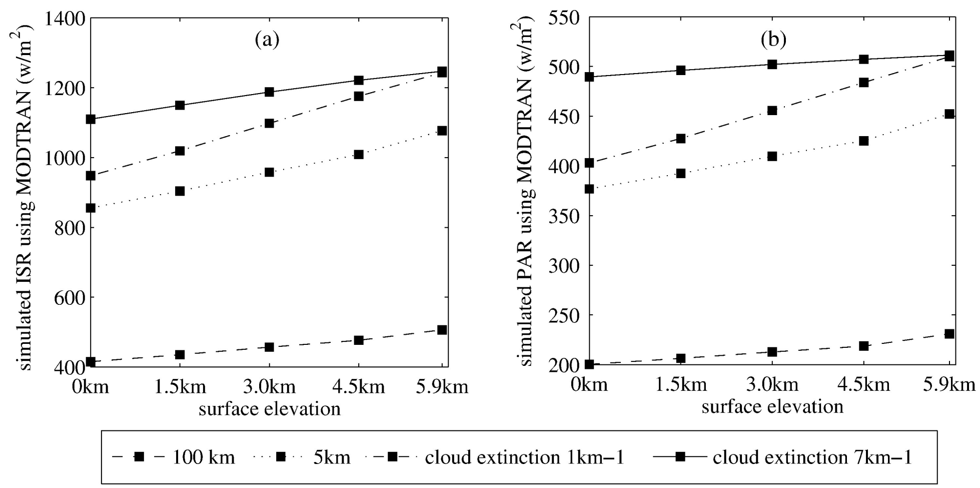

Elevation

Zhang et al., RSE, 2014

Validation of the proposed algorithms

34 field stations of radiative fluxes
24 of them have PAR measurements

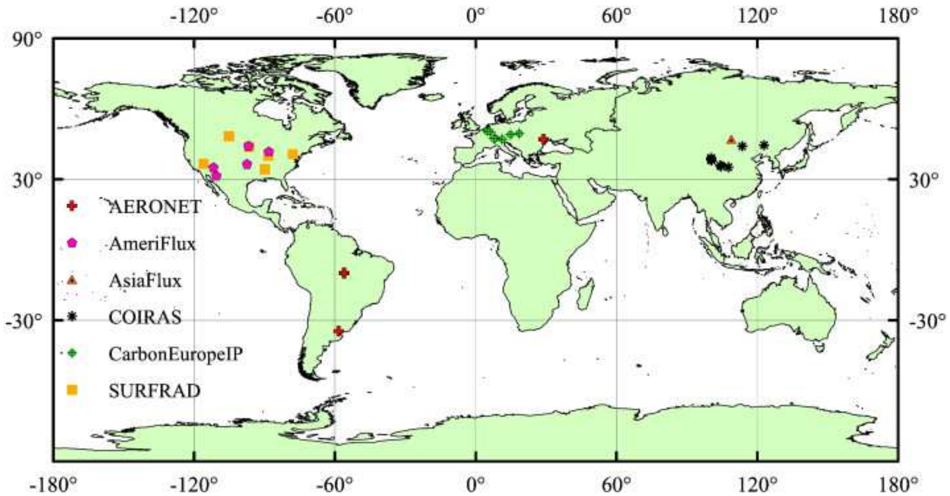

Site	ISR			PAR		
	R^2	BIAS	RMSE	R^2	BIAS	RMSE
Bondville	0.86	20	100	0.86	4.6	45
FortPeck	0.82	5.5	111	0.82	1.6	46
Goodwin Creek	0.92	1.7	86	0.91	4.2	38
Penn State	0.87	12	100	0.86	9.4	44
Sioux Falls	0.86	14	102	0.86	2.4	43
Boulder	0.77	−8.7	140	0.78	−7.6	58
Desert Rock	0.88	−55	119	0.89	−30	51
ARM-SGP Main	0.9	−7.73	93	0.88	16	45
Audubon Research Ranch	0.86	−42	120	0.87	24	56
Brookings	0.83	−9	114	0.84	33	55
Fermi_Agricultural	0.77	55	145	0.78	2	61
Flagstaff Managed Forest	0.78	−26	150	0.77	−19	68
Flagstaff UnManaged Forest	0.86	−24	110	0.88	−4	44
Neustift	0.8	−48	140	0.83	−5	48
Lonzee	0.6	2	131	0.74	9	48
Vielsalm	0.75	12	107	0.79	22	47
Laegeren	0.77	−41	146	0.83	−4	49
Oensingen2 crop	0.77	−10	129	0.86	−9	47
Bily Kriz-Beskidy Mountains	0.77	17	121	0.83	24	48
Bily Kriz grassland	0.79	−3	119	0.82	25	49
[illegible]	[illegible]	[illegible]	[illegible]			
Total	0.83	−6.5	115	0.84	5	49

Site	GLASS ISR			ISCCP-FD			CERES					
							Model B			CCCM enhanced		
	R^2	Bias	RMSE	R^2	Bias	RMSE	R^2	Bias	RMSE	R^2	Bias	RMSE
Bondville	0.87	14.68	104.97	0.71	−7.06	149.88	0.84	12.9	119.5	0.82	−0.5	126.16
FortPeck	0.84	10.51	102.75	0.69	9.61	150.37	0.81	5.3	112.40	0.80	2.3	115.02
Goodwin Creek	0.91	−6.29	99.54	0.64	12.61	184.11	0.69	14.3	172.0	0.66	−3.8	179.35
Penn State	0.85	18.17	109.3	0.7	5.92	152.88	0.87	6.9	107.0	0.86	−8.6	111.18
Sioux Falls	0.81	11.52	114.41	0.65	37.83	168.85	0.62	−11.4	167.4	0.58	−37.8	178.77
Boulder	0.81	−12.8	126.38	0.72	6.49	154.96	0.34	−12.0	249.3	0.47	−43.0	214.41
Desert Rock	0.92	−52.4	112.94	0.87	−42.4	125.27	0.52	−24.2	198.0	0.49	−26.6	206.38

Comparison with existing products

Current status of surface downward radiation product development

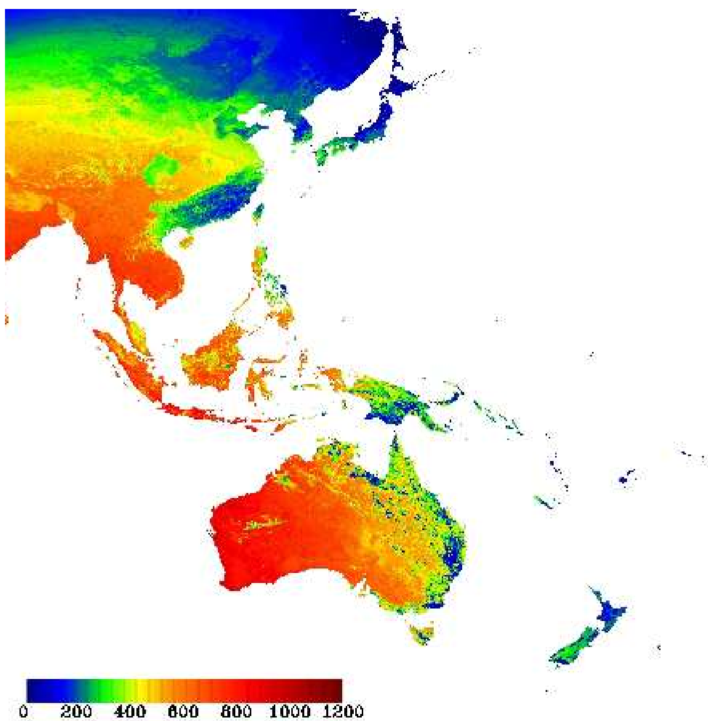

Total land surface shortwave downward radiation (W/m^2) of part of Asia and Oceania on GMT 0530, Jan 2nd, 2010, derived from MODIS and MTSAT data.

Software package:

- Data preprocessing
  - I/O, re-projection, radiometric calibration
- Main algorithm
  - Liang et al. 2006; Zhang et al. 2014
- Data post-processing
  - Data fusion, mosaic
- Ancillary data
  - Water vapor, DEM

ATBD preparation

Estimating surface radiation from hyperspectral data: AVIRIS

- Airborne Visible InfraRed Imaging Spectrometer (AVIRIS) is a airborne hyperspectral sensor.
- It has 224 spectral channels with wavelengths from 400 to 2500 nm.
- AVIRIS is used in NASA HyspIRI Preparatory Airborne Campaign.
- We are funded by NASA to estimate quantities surface radiation budget (including land surface albedo) from HyspIRI-like data.

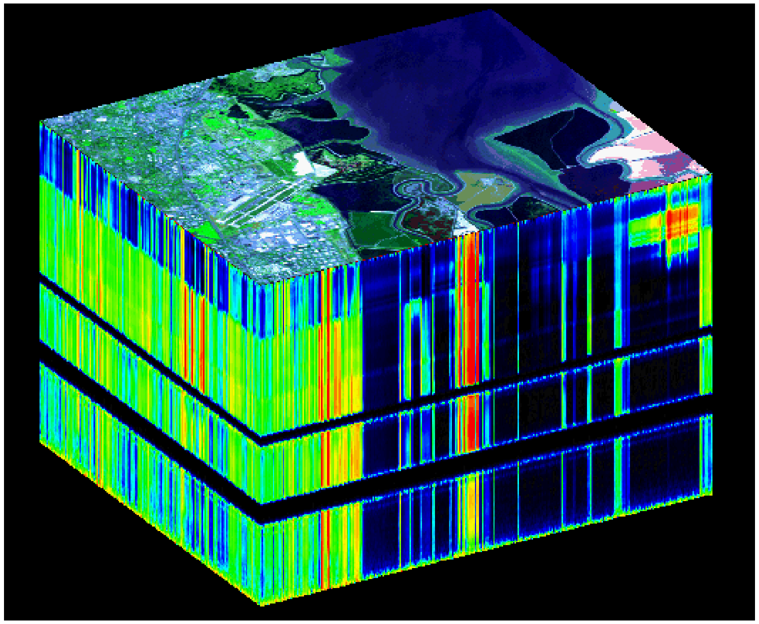

http://aviris.jpl.nasa.gov/data/image_cube.html

Fine-resolution AVIRIS data helps understand uncertainties in validation with scattered clouds in the coarse resolution data

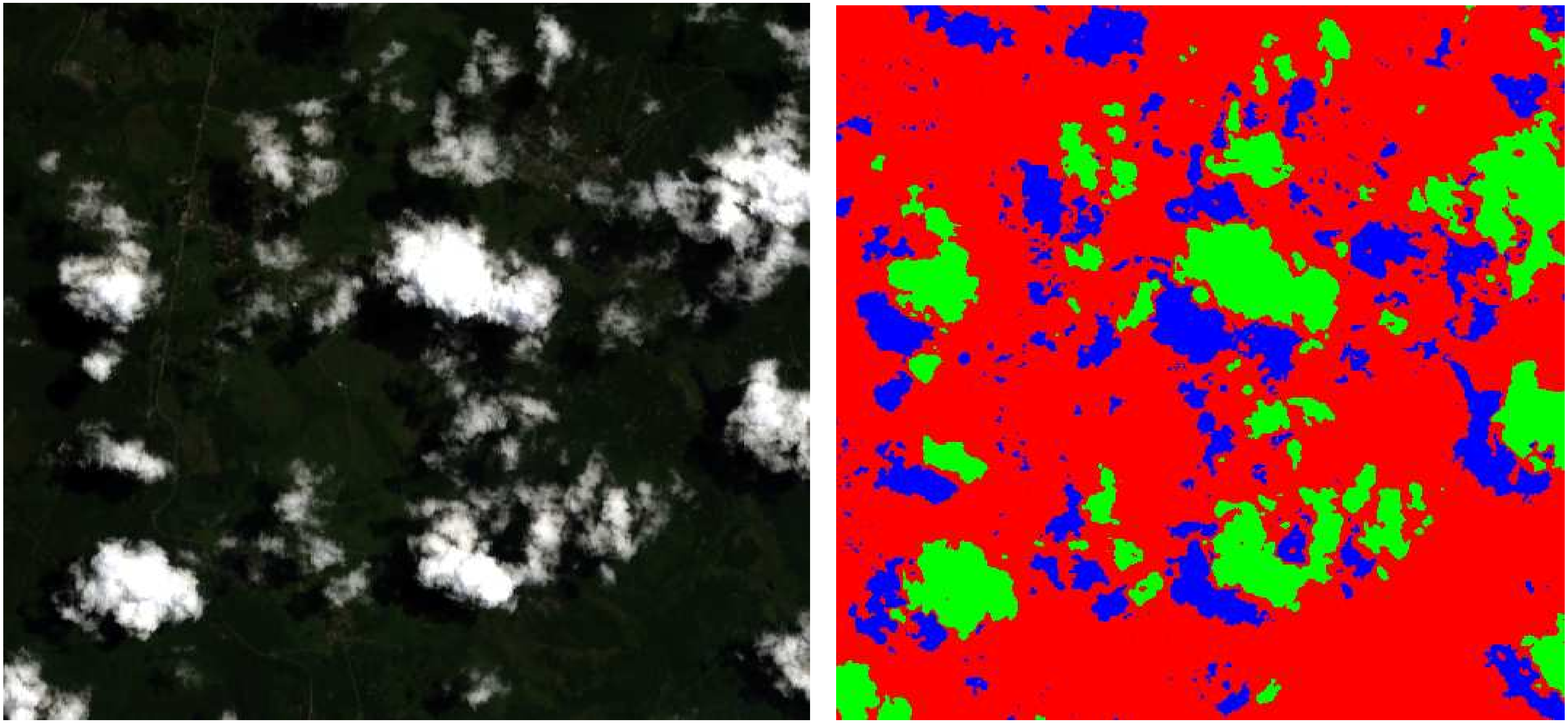

Detection of cloud/shadow from AVIRIS data: (a) True color composite of AVIRIS data at site US-CaV on DOY 187, 2009; (b) detection results of the AVIRIS data (land: red; cloud: green; shadow: blue).

Advantages of hyperspectral information in net shortwave radiation estimation

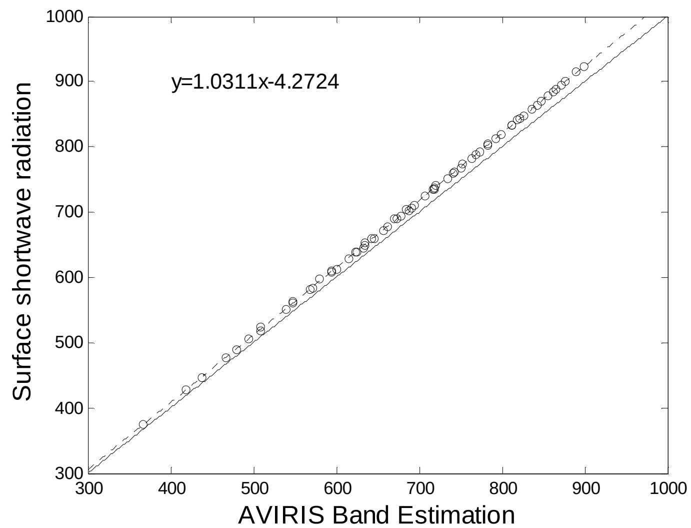

Method A

Conversion of cumulated radiation from AVIRIS bands to shortwave radiation (W/m^2)

Method B

Statistics of NSR direct estimation based on simulation data

RMSE (W/m^2)		Solar zenith angle (°)					
		20	25	30	35	40	45
View zenith angle (°)	0	19.396	19.422	19.394	19.290	19.088	18.768
	5	19.412	19.434	19.429	19.358	19.192	18.906
	10	19.369	19.403	19.397	19.346	19.210	18.954
	15	19.276	19.319	19.312	19.267	19.150	18.921
	20	19.159	19.186	19.184	19.130	19.026	18.815

R^2		Solar zenith angle (°)					
		20	25	30	35	40	45
View zenith angle (°)	0	0.975	0.973	0.970	0.967	0.963	0.957
	5	0.975	0.973	0.970	0.967	0.962	0.957
	10	0.975	0.973	0.970	0.967	0.962	0.956
	15	0.976	0.973	0.971	0.967	0.962	0.957
	20	0.976	0.974	0.971	0.968	0.963	0.957

Estimation surface downward radiation and surface albedo from AVIRIS (Method A): topographic correction

Surface downward radiation

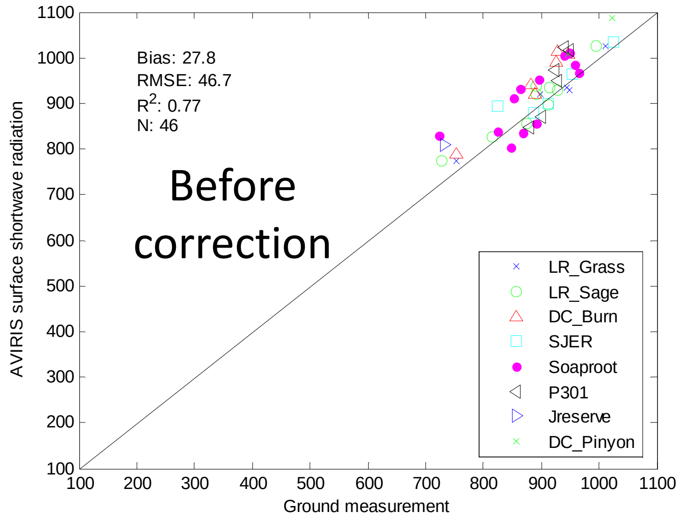

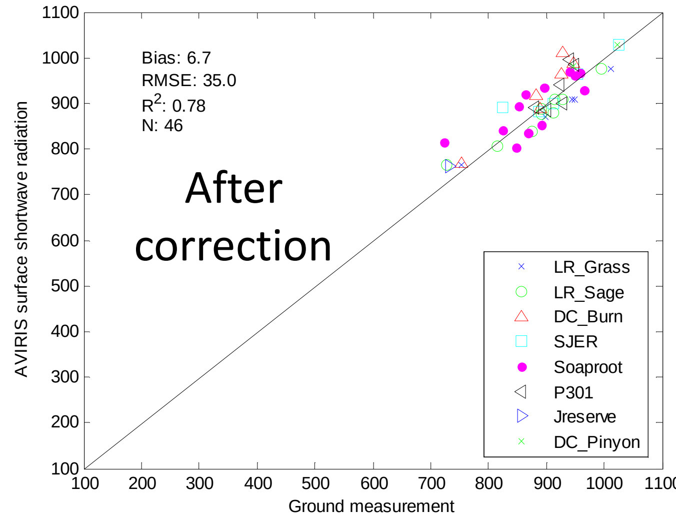

Shortwave albedo before correction

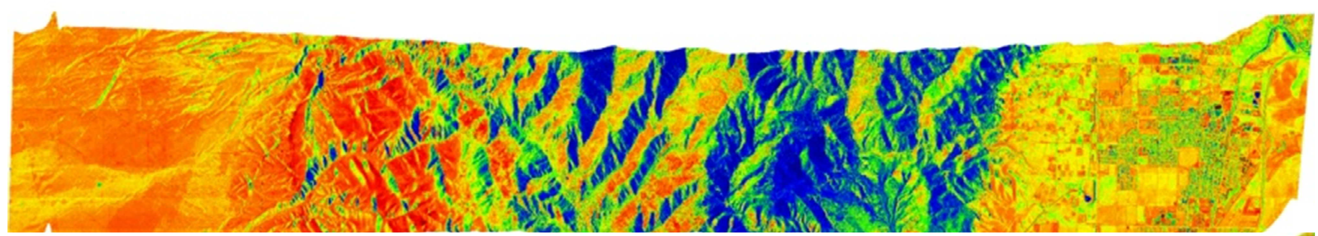

Shortwave albedo after correction

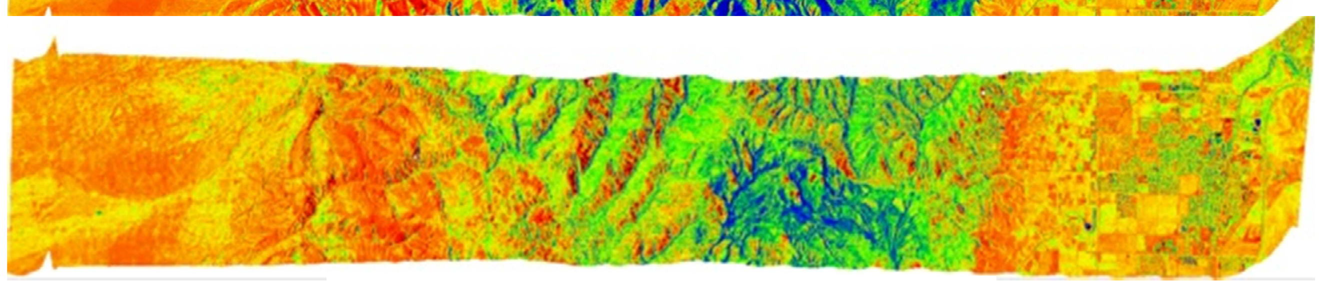

Shortwave downward and net radiation estimation: AVIRIS

(He et al. 2015, *RSE*)

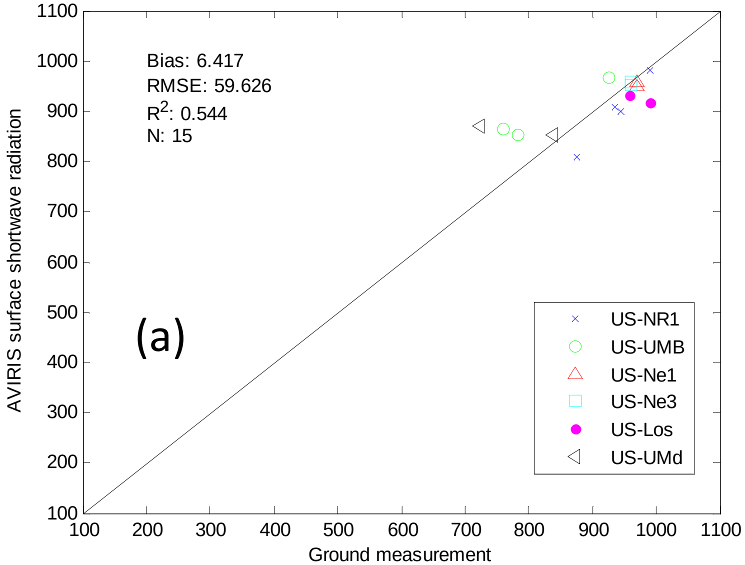

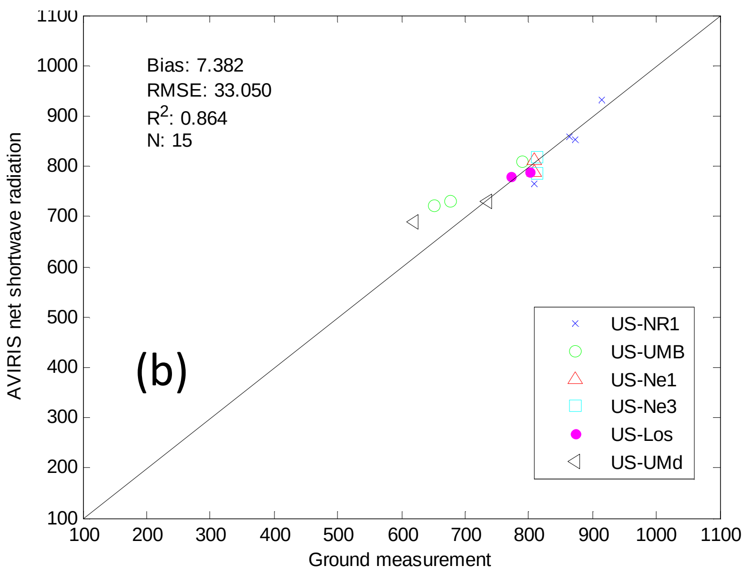

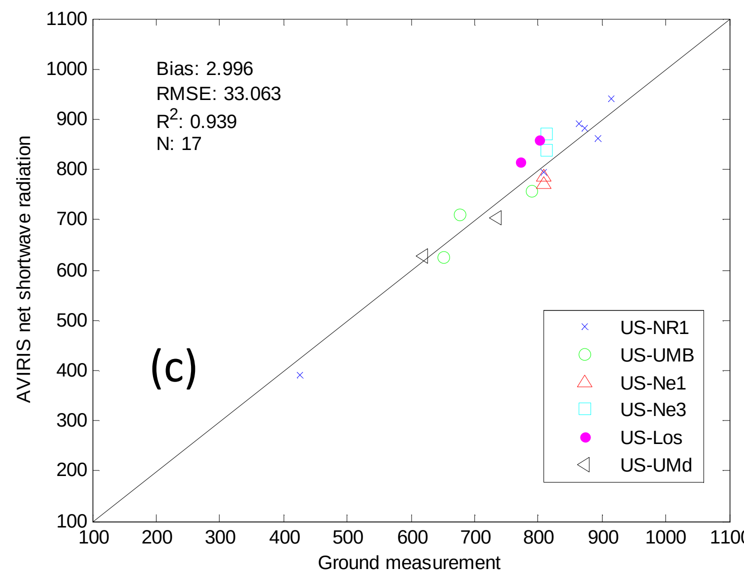

Comparison of ground measurements AVIRIS downward radiation (a) and net radiation from Method A (b) and Method B (c) estimates (W/m^2) at AmeriFlux sites.

Two methods had similar estimation accuracies. N is smaller in (b) than that in (c) because surface albedo estimates were not available under cloud/shadow conditions.

An optimization method for estimating surface downward shortwave radiation

- Assumption
  - Surface BRDF and AOD stay relative stable for a short period of time window.
- Algorithm
  - Simulating atmospheric radiative transfer with Qin’s (2001) non-Lambertian parameterization method
  - Using climatology of BRDF and surface albedo as first guess in optimization
  - Estimating surface downward radiation using the optimized BRDF and AOD as inputs
- Validation
  - One year data of 2005 for 7 SURFRAD sites

Flowchart and Validation

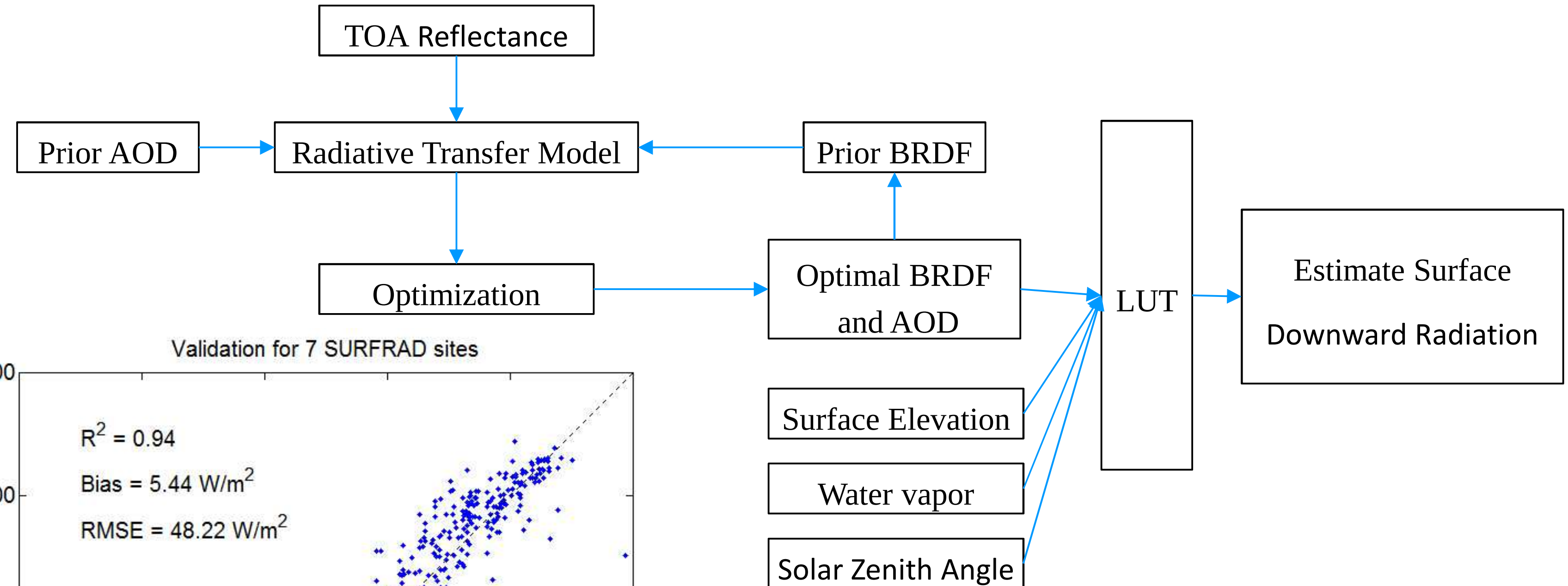

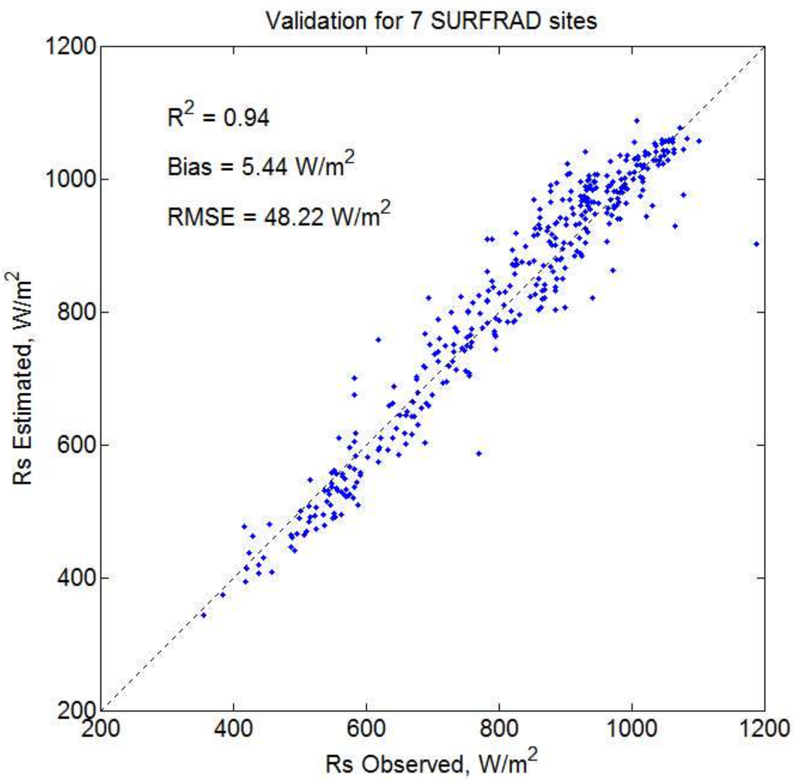

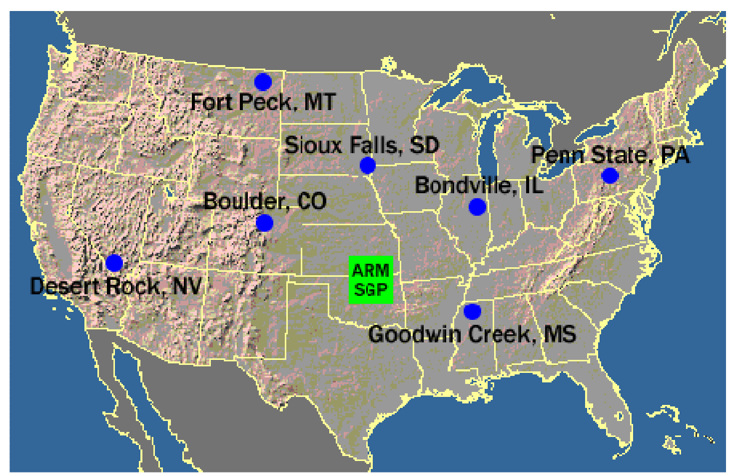

Estimation of daily surface shortwave net radiation (SSNR)

- Shortwave net radiation is equivalent to incident solar radiation, given land surface albedo.
- To develop a more robust high-resolution solar radiation product, we investigated an alternative algorithm for estimating daily shortwave net radiation from MODIS data.
- The morning Terra MODIS data were combined with the afternoon Aqua MODIS data to improve the mapping of intra-daily variations in atmospheric conditions.
- The synergy of the two MODIS sensors reduced the errors in daily SSNR estimates by 6-7 W/m2.

Scale effects in validating SSNR

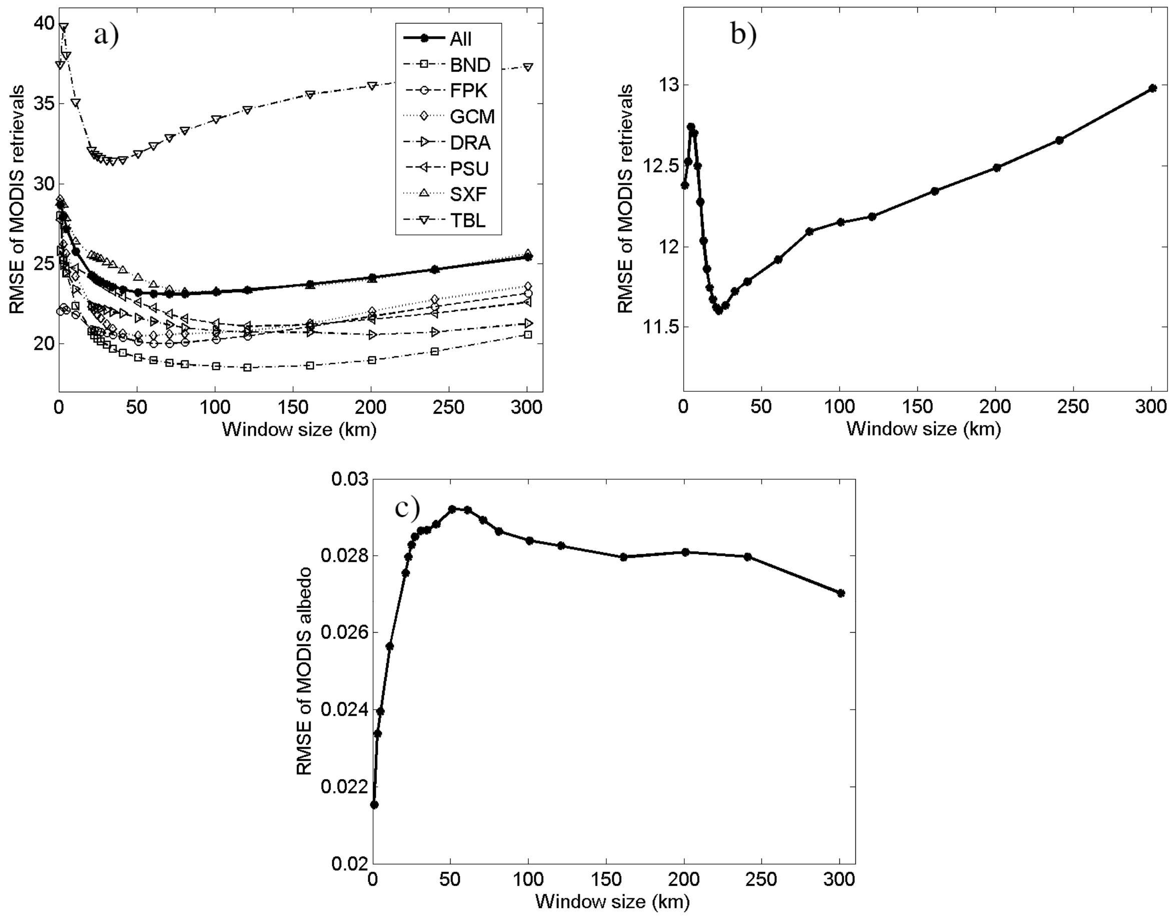

The impacts of window size on the validation results of satellite radiation quantities: a) daily SSNR, b) monthly SSNR and c) surface albedo.

Wang et al. TGRS, in press

Validation results

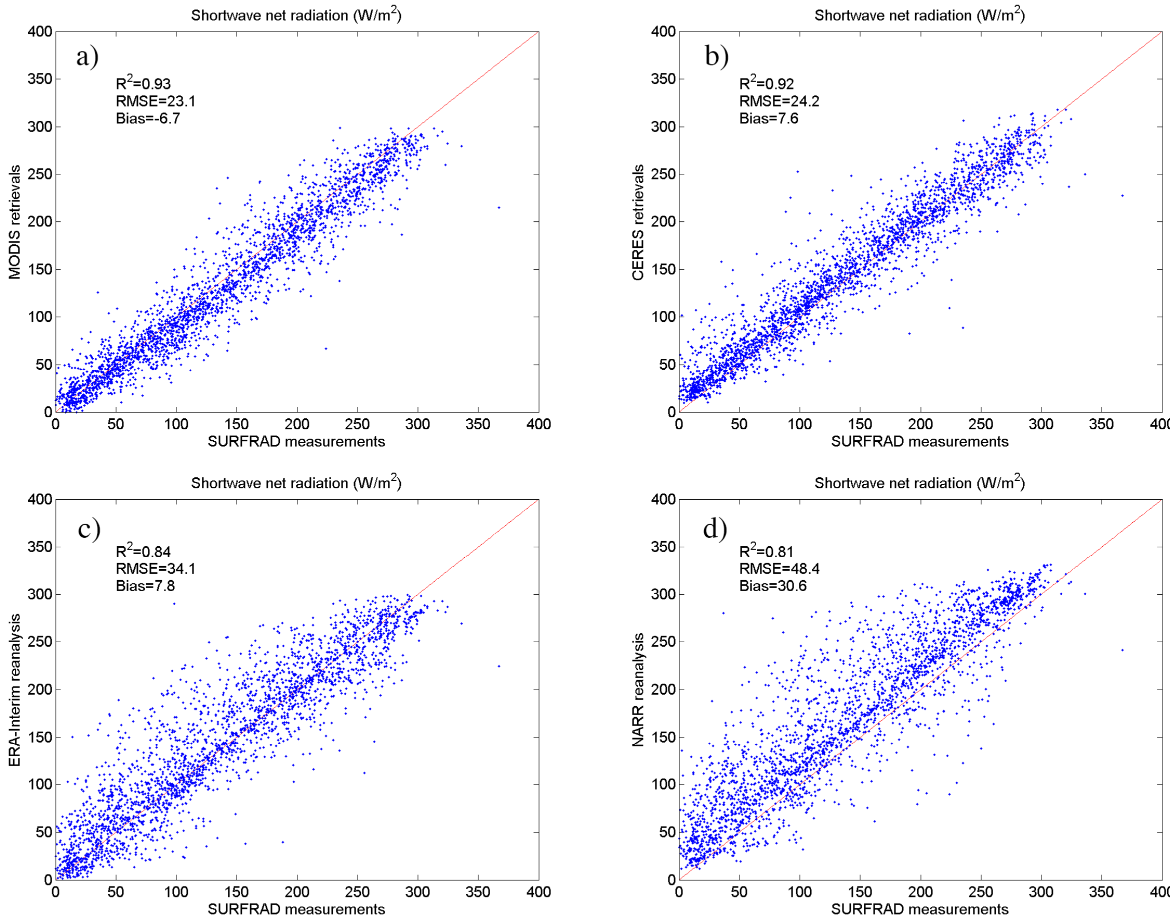

Figure. Comparing field measurements of daily surface shortwave net radiation at seven SURFRAD sites with four data sets: a) MODIS, b) CERES, c) ERA-Interim and d) NARR. MODIS data are averaged from a 71km by 71km window centered at the sites.

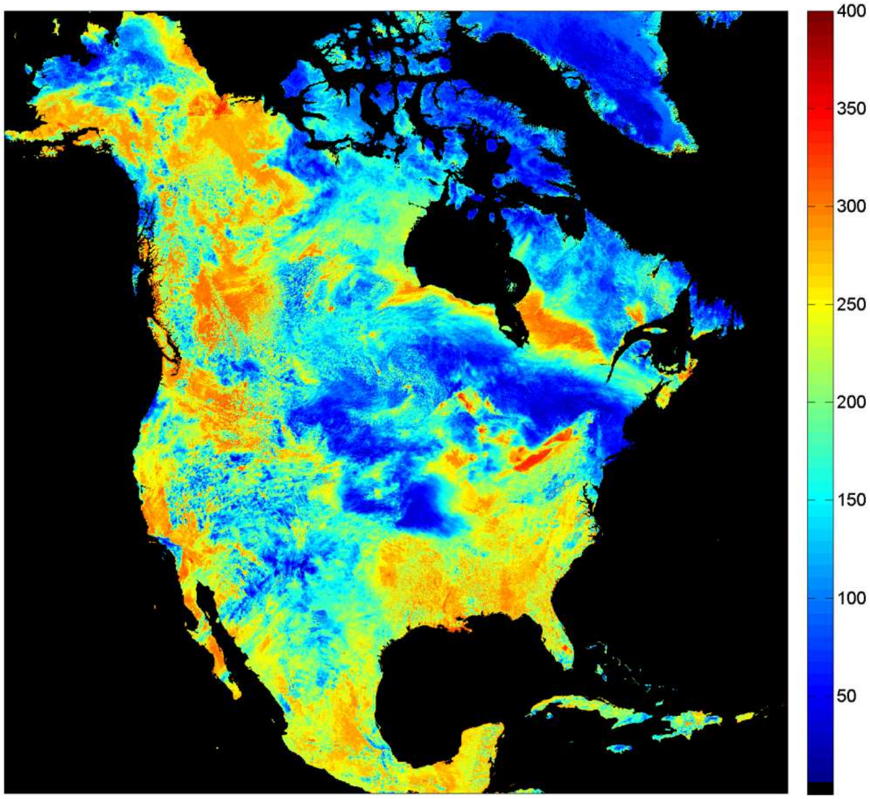

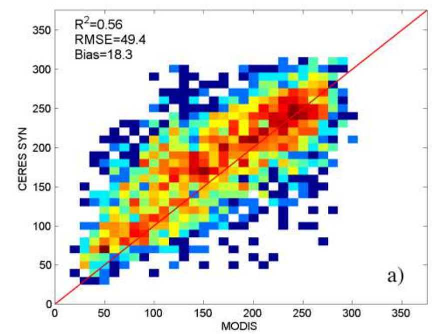

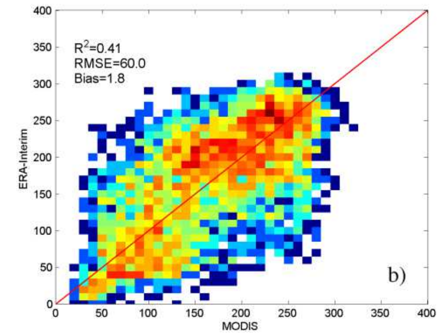

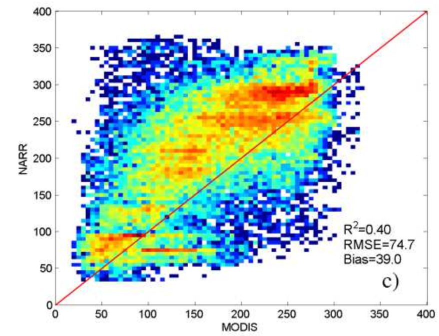

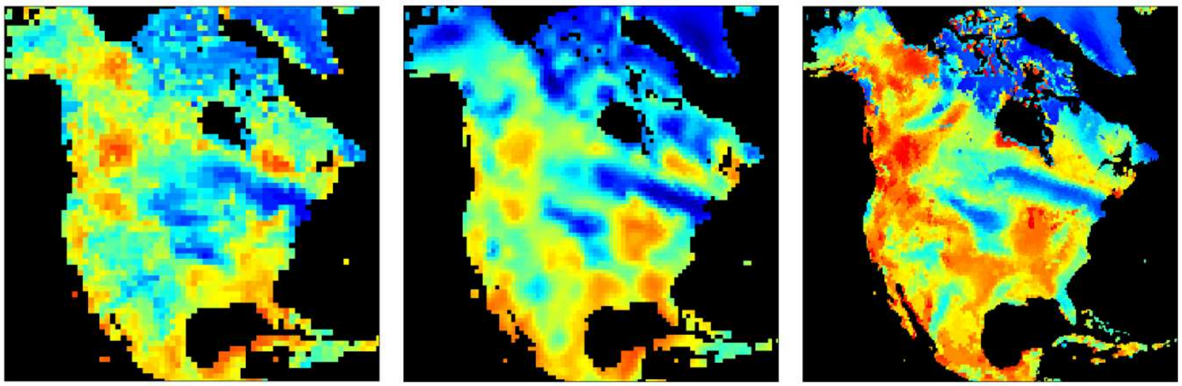

North American maps of daily surface shortwave net radiation on June 9 2009 from a) MODIS, b) CERES) c) ERA-Interim and d) NARR.

Timetable and future work

Tasks	2014-2015				2015-2016				2016-2017			
1. ATBD improvement and code delivery	■	■	■	■	■	■						
2. Evaluation of sensor radiometric calibration	■	■	■	■	■	■						
3. Algorithm validation	■	■	■	■	■	■						
4. Product quality assessment					■	■	■	■	■	■	■	■
5. Product validation					■	■	■	■	■	■	■	■
6. Outreach and product advertisement					■	■	■	■	■	■	■	■

- ATBD and software delivery
- Continuing algorithm improvement
- Extensive algorithm/product validation

Reference

- Wang, D., Liang, S., He, T., & Shi, Q. (2015). Estimation of daily surface shortwave net radiation from the combined MODIS data. IEEE Transactions on Geoscience and Remote Sensing. In press.
- Wang, D., Liang, S., He, T., & Shi, Q. (2015). Estimating clear-sky all-wave net radiation from combined visible and shortwave infrared (VSWIR) and thermal infrared (TIR) remote sensing data. Remote Sensing of Environment. In press.
- He, T., Liang, S.L., Wang, D., Shi, Q., & Goulden, M.L. (2015). Estimation of high-resolution land surface net shortwave radiation from AVIRIS data: algorithm development and preliminary results. Remote Sensing of Environment. In press.
- Wang, D., Liang, S., He, T., Cao, Y., & Jiang, B. (2015). Daily surface shortwave net radiation estimation from FengYun-3 MERSI data. *Remote Sensing, 7*, 6224-6239, doi:10.3390/rs70506224.
- Wang, D. and S. Liang (2014). Mapping High-Resolution Surface Shortwave Net Radiation From Landsat Data. IEEE Geoscience and Remote Sensing Letters 11(2): 459-463.
- Liang, S.L., Zheng, T., Liu, R.G., Fang, H.L., Tsay, S.C., & Running, S. (2006). Estimation of incident photosynthetically active radiation from Moderate Resolution Imaging Spectrometer data. Journal of Geophysical Research-Atmospheres, 111
- Zhang, X.T., Liang, S.L., Zhou, G.Q., Wu, H.R., & Zhao, X. (2014). Generating Global LAnd Surface Satellite incident shortwave radiation and photosynthetically active radiation products from multiple satellite data. Remote Sensing of Environment, 152, 318-332

Summary

- The major tasks have been performed as scheduled.
- We expect to deliver the codes and ATBD by the end of this year.
- We have investigated several related issues and explored new methods for further improvement:
  - Scaling issues in validation;
  - New optimization method;
  - Application of hyperspectral data;
  - Temporal scaling of daily SSNR.